HHS Public Access

Author manuscript

Science. Author manuscript; available in PMC 2024 June 17.

Published in final edited form as:

Science. 2023 November 10; 382(6671): 725–731. doi:10.1126/science.adh0037.

Histone removal in sperm protects paternal chromosomes from premature division at fertilization

Raphaälle Dubruille[1,*,†], **Marion Herbette**[1,†,‡], **Maxime Revel**[1,§], **Béatrice Horard**[1], **Ching-Ho Chang**[2], **Benjamin Loppin**[1,*]

[1]Laboratoire de Biologie et Modélisation de la Cellule, École Normale Supérieure de Lyon, CNRS UMR5239, Université Claude Bernard Lyon 1, Lyon, France

[2]Division of Basic Sciences, Fred Hutchinson Cancer Center, Seattle, WA, USA

Abstract

The global replacement of histones with protamines in sperm chromatin is widespread in animals, including insects, but its actual function remains enigmatic. We show that in the *Drosophila* paternal effect mutant *paternal loss* (*pal*), sperm chromatin retains germline histones H3 and H4 genome wide without impairing sperm viability. However, after fertilization, *pal* sperm chromosomes are targeted by the egg chromosomal passenger complex and engage into a catastrophic premature division in synchrony with female meiosis II. We show that *pal* encodes a rapidly evolving transition protein specifically required for the eviction of $(H3\text{-}H4)_2$ tetramers from spermatid DNA after the removal of H2A-H2B dimers. Our study thus reveals an unsuspected role of histone eviction from insect sperm chromatin: safeguarding the integrity of the male pronucleus during female meiosis.

Introduction

Sperm chromatin is generally characterized by a high level of DNA compaction, which reduces nuclear volume and contributes to the shape and hydrodynamic properties of the sperm head (1, 2). In many animal species, tight packaging of sperm DNA follows the replacement of nucleosomal histones with sperm nuclear basic proteins (SNBPs), such as the well-characterized mammalian protamines (3). This distinct, global chromatin remodeling process known as the histone-to-protamine transition occurs during spermiogenesis, the differentiation of post-meiotic spermatids (1, 2, 4). Although the histone-to-protamine transition is generally assumed to be essential for the formation of functional sperm, not

[*]Corresponding author. raphaelle.renard-dubruille@ens-lyon.fr (R.D.); benjamin.loppin@ens-lyon.fr (B.L.).
[†]These authors contributed equally to this work.
[‡]Present address: Institute of Ecology and Evolution, University of Edinburgh, Edinburgh, UK.
[§]Present address: Department of Genetics, University of Geneva, Geneva, Switzerland.

Author contributions: Conceptualization: R.D., C.-H.C., and B.L.; Methodology: R.D., M.H., C.-H.C., B.H., and B.L.; Investigation: R.D., M.H., M.R., B.H., C.-H.C., and B.L.; Visualization: R.D., M.H., C.-H.C., B.H., and B.L.; Funding acquisition: R.D., C.-H.C., and B.L.; Supervision: R.D. and B.L.; Writing – original draft: B.L.; Writing – review and editing: R.D., M.H., B.H., C.-H.C., and B.L.

Competing interests: The authors declare that they have no competing interests.

all animals use SNBPs for sperm chromatin assembly. For example, whereas mammalian sperm DNA is mostly packaged with protamines, many other vertebrates maintain a full nucleosome-based sperm chromatin (5, 6). Even within groups of related species (e.g., teleost fishes), sperm chromatin can vary between protamine based and histone based (7, 8). These repeated transitions between nucleosomal and nucleoprotamine sperm chromatin (3, 9) have left the function of histone replacement by SNBPs unclear.

Despite their enormous diversity and ancient evolutionary history, all major orders of insects consistently encode “histone-free” packaging of sperm DNA (10–12). As the best characterized example, the model species *Drosophila melanogaster* has ultracompact sperm chromatin entirely organized with protamine-like SNBPs, except for centromeres that retain the centromeric histone H3 (CenH3) (1, 4, 13). This indicates that a stringent selective requirement for SNBP-based sperm chromatin must exist in insects. In this work, we discovered that the replacement of histones with SNBPs is functionally linked to a postfertilization process through the characterization of a *Drosophila* paternal effect mutant named *paternal loss* (*pal*).

Results

Paternal effect mutants represent a rare genetic resource to investigate sperm functions that are specifically required for the integration of paternal chromosomes in the zygote (14–18). The *pal* mutant, which was isolated more than fifty years ago, has been known to induce sporadic loss of paternal chromosomes at the onset of embryonic development (14, 19, 20), but the origin of this phenotype is unknown. In wild-type eggs fertilized by sperm from *pal* mutant males, loss of the paternal X chromosome, for example, occurs in about 3% of adult progeny and can lead to the development of bilateral gynandromorphs, with half male (X0) and half female (XX) tissues (20) (Fig. 1A). Similarly, losses of the Y chromosome and the small chromosome 4, but not one of the larger, essential chromosomes 2 or 3, were also detected in the progeny of *pal* males (14, 20). To investigate the cytological bases of these early chromosome losses, we collected wild-type eggs fertilized by sperm from *pal* mutant males (hereafter referred to as *pal* eggs). In *Drosophila*, after fertilization, the male and female pronuclei migrate to a central region of the egg where they appose without fusing their nuclear envelopes (Fig. 1B). We observed frequent (~50 to 60%; table S1) fragmentation of the male pronucleus at the apposition stage in *pal* eggs (Fig. 1C). As expected, this phenotype was followed by the sporadic loss or fragmentation of paternal chromosomes during the first and second embryonic mitoses (Fig. 1, D and E), which was in agreement with Baker’s original prediction based on adult mosaic analyses (20). In addition, we observed that about half of *pal* eggs did not hatch (table S2), suggesting that most of these early chromosomal defects cause embryonic arrest. Taken together, these observations indicate that loss of paternal chromosomes in *pal* eggs is a secondary consequence of a much more penetrant phenotype that affects the integrity of the male pronucleus.

Paternal chromosomes in *pal* eggs are aberrantly targeted by the CPC

We investigated the cause of male pronuclear fragmentation in *pal* eggs. In contrast to most vertebrates in which fertilization occurs in oocytes arrested in metaphase II of female

meiosis, insect fertilization occurs when female meiosis resumes from metaphase I arrest (21–26). In *Drosophila*, the earliest stage of fertilized eggs practically accessible to cytology is metaphase II, which is recognized by the presence of the female meiotic spindles organized in tandem (Fig. 1B). At this stage, in eggs fertilized by wild-type sperm (referred to as wild-type eggs), the sperm nucleus has already replaced its SNBPs with histones and typically appears as a small, roundish nucleus. We found that in *pal* eggs, the male nucleus was irregular in shape and almost systematically surrounded by a spindle of microtubules (96.4%, $n = 28$; Fig. 1F). Such ectopic, paternal spindles were not observed in wild-type eggs (0%, $n = 36$). Like female meiotic spindles, the paternal spindle in *pal* eggs was anastral (Fig. 1F) and sperm-derived centrioles were normally found in the sperm aster, a large aster of microtubules that captures the female pronucleus (fig. S1). The paternal pseudodivision progressed in synchrony with female meiosis II and the paternal chromatids derived from the haploid sperm nucleus eventually stretched between the spindle poles (Fig. 1F). This suggests that paternal chromosomes in *pal* eggs follow the same cytoplasmic cues that control female meiosis progression. We thus investigated whether the pseudodivision of *pal* paternal chromosomes is triggered by the chromosomal passenger complex (CPC), which controls meiotic spindle formation in *Drosophila* oocytes by enabling kinetochore assembly and microtubule recruitment (27). A key subunit of the CPC is the Aurora B kinase, which phosphorylates histone H3 on serine 10 (H3S10ph) (28). In wild-type eggs in meiosis II, H3S10ph was exclusively found on maternal chromosomes ($n = 21$; Fig. 1F). By contrast, in *pal* eggs, this histone mark decorated both maternal and paternal chromosomes (100%, $n = 15$; Fig. 1F). Consistently, INCENP, another CPC subunit (27), also aberrantly localized on paternal chromosomes and the paternal spindle in *pal* eggs (fig. S1). To demonstrate that the CPC was responsible for the cytological defects affecting the male pronucleus in *pal* eggs, we crossed *pal* males with females expressing a small hairpin RNA targeting *aurora B* (*aurB*) in the germline. As expected, maternal knockdown (KD) of *aurB* abolished phosphorylation of H3S10 on female chromosomes and prevented meiosis progression (fig. S2). In *aurB* KD eggs fertilized with *pal* sperm, we additionally observed a complete suppression of the *pal* pronuclear phenotype (fig. S2). We conclude that in *pal* eggs, the CPC instructs the paternal genome to engage in a pseudomeiotic division, leading to frequent pronuclear fragmentation and occasional losses of paternal chromosomes.

Histones H3 and H4 are aberrantly retained in *pal* sperm chromatin

Because *pal* is a paternal effect mutant, we investigated whether these egg phenotypes may result from an altered sperm chromatin organization. In *Drosophila*, the histone-to-protamine transition occurs at midspermiogenesis and noncentromeric histones are replaced with protamine-like SNBPs before the individualization of spermatids (1). *Drosophila* comprises a minimal set of nucleosome core histones, including canonical (or replicative) histones H2A, H2B, H3.2, and H4, and histone variants H2Av, H3.3, and Cid/CenH3 (29). We found that transgenic red fluorescent protein (RFP)–tagged H2A, H2Av, and H2B expressed in the male germline were completely removed from spermatid nuclei at the histone-to-protamine transition in control and *pal* testes (Fig. 2, A and B, and fig. S3, A and B). By contrast, although green fluorescent protein (GFP)–tagged H3.2 and H3.3 were also removed in control males, both transgenic H3 histones were aberrantly retained in *pal* mutants, marking all sperm nuclei (Fig. 2C and fig. S3C). Our immunofluorescence analyses also revealed

the persistence of acetylated H4 (H4ac) beyond the histone-to-protamine transition in *pal* testes (fig. S3D), thus suggesting that histones are retained as $(H3\text{-}H4)_2$ tetramers on sperm DNA (tetrasomes) following the partial disassembly of nucleosomes. We observed that GFP-Cid, the *Drosophila* centromeric H3 that is retained in mature sperm (13), was normally distributed as four foci in *pal* sperm nuclei (fig. S3E). These results imply that, during normal *Drosophila* spermiogenesis, the removal of H2A-H2B dimers from spermatid nucleosomes is functionally uncoupled from the final elimination of $(H3\text{-}H4)_2$ tetramers. To directly examine the dynamics of histone removal in transitioning spermatid nuclei, we simultaneously imaged H2A-RFP and H3.3-GFP and measured relative fluorescence intensities in spermatid cysts at different stages. We found that the disassembly of spermatid nucleosomes is a sequential process, with H2A-H2B dimers being eliminated first, followed by histones H3 and H4 (fig. S4). Notably, global retention of H3 and H4 in *pal* spermatozoa did not preclude loading of the major *Drosophila* SNBPs Protamine B (ProtB) and Mst77F (Fig. 2D and fig. S3A). However, western blot quantification of ProtB-GFP suggested that SNBPs are less abundant in *pal* sperm than in control sperm (fig. S5). Although *pal* sperm nuclei appeared regular and homogeneous in shape, they were on average 25% shorter and significantly wider than wild-type sperm nuclei (Fig. 2, D and E). This difference had no apparent impact on the motility or fertilization potential of *pal* gametes (Movie S1 and fig. S6), revealing the remarkable plasticity of *Drosophila* spermatozoa with respect to their chromatin composition and nuclear morphology. We conclude that the *pal* gene is specifically required for the elimination of H3 and H4 at the histone-to-protamine transition.

pal sperm rescues the viability of *Hira* mutant eggs

We then sought to evaluate the actual contribution of *pal* sperm histones to paternal nucleosome reassembly after fertilization. Crossing H3.3-GFP–expressing *pal* males with wild-type females revealed that H3.3-GFP specifically decorated paternal chromatin in the male pronucleus and throughout the first zygotic division (100%, $n = 18$; Fig. 3A). Thus, paternally transmitted histones in *pal* sperm directly contribute to the formation of paternal nucleosomes in the egg. We then wondered whether maternal H3 and H4 histones stored in the egg are nevertheless required for male pronuclear formation in *pal* eggs. In both vertebrates and invertebrates, genome-wide histone deposition on paternal DNA following SNBP removal is initiated by the conserved HIRA histone chaperone complex (30). Specifically, maternal HIRA assembles $(H3.3\text{-}H4)_2$ tetramers in the male pronucleus in a replication-independent manner. In the absence of functional HIRA, such as in the *Drosophila* maternal effect mutant *sésame* (*Hira*^{ssm}), fertilized eggs fail to initiate paternal nucleosome assembly and develop only with maternal chromosomes, which leads to haploid development and full embryonic lethality (31, 32). We observed that crosses between *Hira*^{ssm} females and *pal* males were fertile, with embryo hatching at rates on par with that of control crosses involving *pal* males and wild-type females (Fig. 3B and table S2). In addition, both crosses produced a similar number of adult progenies (Fig. 3C), and *pal* males were also able to restore the fertility of females with germline knockdown of *Hira* (table S2). At the cytological level, instead of the typical *Hira*^{ssm} phenotype showing a round, inert male pronucleus, *Hira*^{ssm} eggs fertilized by *pal* sperm showed only a *pal* phenotype, demonstrating that *pal* is epistatic to *Hira*^{ssm} (Fig. 3D). This suggests that, in *pal* sperm chromatin, H3 and H4 are present as tetrasomes throughout the paternal genome, thus

bypassing the need for HIRA during male pronuclear formation. To determine the timing of paternal nucleosome reconstitution in *pal* eggs, we crossed *pal* mutant males with transgenic females expressing H2A-RFP. Maternal H2A-RFP decorated the male pronucleus of *pal* eggs as early as meiosis II (100%, $n = 13$) in a way indistinguishable from that of control eggs (100%, $n = 11$) (Fig. 3E). This result confirms that in *pal* eggs, H2A-H2B dimers stored in the egg cytoplasm are deposited on sperm tetrasomes in a replication-independent manner.

We conclude that the persistence of H3-H4 in *pal* sperm establishes an aberrant epigenetic identity of paternal chromosomes at fertilization, ultimately leading to their incorrect recognition by the CPC as maternal chromosomes during the second female meiotic division.

pal encodes a fast-evolving transition protein

To identify the *pal* gene, we performed a classical deficiency mapping of the original pal^1 allele (19,20). We narrowed down the *pal* locus to a 76-kb interval in region 30C of chromosome 2L (Fig. 4A and table S1; see the supplementary text). Across this region, whole-genome sequencing of pal^1 flies identified a nonsense point mutation in *CG31882*, a small, intronless gene specifically expressed in testes and predicted to encode a 121–amino acid (aa) basic protein (Fig. 4B and fig. S7). The premature stop codon in pal^1 leads to 30-aa C-terminal truncation of CG31882 protein. To validate that *CG31882* is indeed *pal*, we generated a deletion that removes most of *CG31882* coding region with CRISPR-Cas9. The deletion, named $pal^{\Delta 4}$, recapitulated the phenotypes of *pal* eggs (Fig. 4B and table S2). By contrast, we found that a previously reported insertion-deletion allele, $CG31882^{RT4}$ (33), which likely causes changes in the N terminus of the protein, did not impair *pal* function (fig. S7; see supplementary text). We also generated transgenes expressing wild-type Pal or Pal tagged with V5 (Pal-V5) under the endogenous regulatory regions of *pal* (Fig. 4B), which rescued the cytological defects of *pal* eggs (table S1). Both transgenes also restored full embryo lethality in crosses with $Hira^{ssm}$ females (table S2), thus confirming that the *CG31882* is the pal gene and demonstrating that Pal-V5 is functional.

At the cytological level, in testes, we observed that Pal-V5 transiently accumulates in spermatid nuclei undergoing the histone-to-protamine transition (Fig. 4, C and D). Pal-V5 first appeared in spermatids that had begun to incorporate the transition protein Tpl94D (10) and were still positive for H4ac (Fig. 4, C and E). Pal-V5 was still detectable shortly after H4ac disappearance but vanished before that of Tpl94D (Fig. 4, D to E). We thus conclude that Pal is a transition protein required for histone H3 and H4 eviction before the final deposition of SNBPs (Fig. 4F).

Previous analyses had suggested that *CG31882* is an evolutionarily young, testis-specific gene limited to species of the *D. melanogaster* subgroup, identified through sequence homology searches (33–35). However, our examination of syntenic regions flanked by *GlcAT-S* and *Apoltp* revealed orthologs of this gene in most surveyed *melanogaster* group species as well as in other Drosophilinae subfamily species (Fig. 4G and fig. S8A). RNA sequencing analyses further confirmed their testis- or male-specific expression (table S3). Comparison of the different *pal* orthologs reveals that its protein evolutionary rate [the

nonsynonymous substitution rates (dN) normalized by synonymous substitutions rates (dS)] in the *D. melanogaster* subgroup is higher than that of most genes, including known SNBPs (fig. S8B) (36, 37). Although we did not detect any positively selective sites using the site model in PAML ($P = 0.59$), the highly divergent Pal proteins share a conserved 20-aa motif at their C terminus (Fig. 4G). This motif, which is truncated in the pal^1 allele, is thus likely of critical importance for Pal function. In some *melanogaster* group species, such as *D. ananassae, pal* orthologs are apparently absent despite their conservation in more divergent species (Fig. 4G). Our findings are reminiscent of another study in *Drosophila* in which it was found that young, rapidly evolving SNBP genes are more likely to encode important functions than older, evolutionarily constrained genes (37). Thus, even though the histone eviction function is critical, the genetic means by which this function is mediated may vary across *Drosophila* and other insect species.

Discussion

Paternal effect mutants represent invaluable genetic tools to investigate the influence of spermiogenesis and sperm chromatin composition on the fate of paternal chromosomes at fertilization. In *Drosophila*, the molecular characterization of *K81* (15, 38) and *deadbeat* (17) has, for example, revealed that these paternal gene products establish an epigenetic protection of sperm telomeres in the egg. Similarly, Heterochromatin Protein 1E exerts a transgenerational effect on the integrity of paternal chromosomes during the first mitosis (16). The elucidation of the *pal* phenotype now sheds light on the role of sperm histone elimination as an adaptation to constraints exerted by the egg cytoplasm on the fertilizing sperm nucleus.

Our characterization of *pal* first reveals the extraordinary plasticity of insect sperm chromatin composition. Although *Drosophila* spermiogenesis is sensitive to the loss of particular SNBPs (39–41), the global retention of H3 and H4 histones observed in *pal* mutants has no detectable impact on sperm differentiation or function despite substantial changes in nuclear morphology. It suggests that major diversification of sperm chromatin composition in animals could result from minimal changes in genes involved in the histone-to-protamine transition.

In *pal* sperm, we hypothesize that $(H3\text{-}H4)_2$ tetramers are distributed throughout the genome, reflecting the original position of nucleosomes before the removal of H2A and H2B at the histone-to-protamine transition. These tetrasomes must then coexist with SNBPs that are subsequently deposited, although less abundantly than in normal sperm chromatin. Incidentally, this study also establishes that histone elimination during *Drosophila* spermiogenesis is a sequential process, with the removal of H2A-H2B and H3-H4 being temporally and functionally distinct. Notably, during mouse spermiogenesis, the replacement of H2A and H2B with testis-specific histone variants prepares the final replacement of nucleosomes with protamines (42–44), whereas in *Xenopus*, only H2A-H2B dimers are partially replaced with SNBPs, leading to the retention of H3 and H4 in sperm (45). The sequential elimination of histones in spermatids could thus be widespread in animals.

The recurrent packaging of sperm DNA with nonhistone proteins is a longstanding mystery in chromatin biology and evolution. Main hypotheses on this specialization include sperm nuclear compaction, transcriptional shutdown in spermatids, and sperm DNA protection against damages (5, 44, 46). Our work now suggests that the timing of egg fertilization with respect to female meiosis progression is a previously unexplored, key determinant of sperm chromatin evolution in animals. In insects, early fertilization (metaphase of meiosis I) inevitably exposes the decondensing sperm nucleus to egg cytoplasmic cues that initiate the second meiotic division of maternal chromosomes. We propose that the global and invariable replacement of histones with SNBPs in insects establishes an epigenetic identity of paternal chromosomes that prevents their deleterious interaction with the egg CPC. In vertebrate eggs, the relatively late oocyte fertilization timing (metaphase of meiosis II) may offer a more permissive environment to the fertilizing sperm nucleus during its transformation into a pronucleus. In support of this possibility, premature chromosome condensation of sperm chromosomes, a defect highly reminiscent of the *pal* phenotype, is frequently observed when in vitro fertilization or intracytoplasmic sperm injection is performed with immature mammalian oocytes (47, 48). The temporal uncoupling of female meiosis II initiation and male pronuclear formation in vertebrates could have thus favored the extreme diversification of sperm chromatin types, including histone-based sperm chromatin. Still, other animals with an early type of fertilization, such as the model nematode *Caenorhabditis elegans*, maintain histone-based sperm chromatin (49), which suggests the evolution of additional, yet unknown mechanisms to protect the paternal genome during the formation of the diploid zygote.

Supplementary Material

Refer to Web version on PubMed Central for supplementary material.

ACKNOWLEDGMENTS

We thank H. S. Malik, M. Francesconi, and M. Delattre for their helpful comments and suggestions on the manuscript. We are grateful to E. C. Lai, K. McKim, and the Bloomington Drosophila Stock Center for antibodies and fly stocks. We also thank S. Suchet for the initial observation that *pal* males rescue the fertility of *Hira*^{ssm} females, M. Caron for plasmid constructions, and J. Brocard for his help with movie recording. We acknowledge the contribution of the Lyon SFR Biosciences (UAR3444/CNRS, US8/INSERM, ENS de Lyon, UCBL) imaging facility (PLATIM) and fly food production (Arthrotools).

Funding:

This work was supported by French National Research Agency grants ANR-16-CE12-0006-01 (R.D.) and ANR-21-CE13-0037 (B.L.) and Damon-Runyon Cancer Research Foundation postdoctoral fellowship DRG 2438-21 (C.-H.C.). C.-H.C. is also supported by a National Institutes of Health grant R01-GM74108 to H. S. Malik.

Data and materials availability:

All data are available in the main text or the supplementary materials. Fly stocks and plasmids are available upon request.

REFERENCES AND NOTES

1. Rathke C, Baarends WM, Awe S, Renkawitz-Pohl R, Biochim. Biophys. Acta 1839, 155–168 (2014). [PubMed: 24091090]

2. Moritz L, Hammoud SS, Front. Endocrinol. (Lausanne) 13, 895502 (2022). [PubMed: 35813619]
3. Lewis JD, Song Y, de Jong ME, Bagha SM, Ausió J, Chromosoma 111, 473–482 (2003). [PubMed: 12743711]
4. Hao S-L, Ni F-D, Yang W-X, Gene 706, 201–210 (2019). [PubMed: 31085275]
5. Balhorn R, Genome Biol. 8, 227 (2007). [PubMed: 17903313]
6. Ausió J, González-Romero R, Woodcock CL, J. Struct. Biol 188, 142–155 (2014). [PubMed: 25264147]
7. Saperas N, Ribes E, Buesa C, García-Hegart F, Chiva M, J. Exp. Zool 265, 185–194 (1993). [PubMed: 8423442]
8. Wu S-F, Zhang H, Cairns BR, Genome Res. 21, 578–589 (2011). [PubMed: 21383318]
9. Eirín-López JM, Ausió J, BioEssays 31, 1062–1070 (2009). [PubMed: 19708021]
10. Rathke C et al., J. Cell Sci 120, 1689–1700 (2007). [PubMed: 17452629]
11. Ferree PM et al., Sci. Rep 9, 12194 (2019). [PubMed: 31434920]
12. Orsi GA et al., Nat. Commun 14, 4187 (2023). [PubMed: 37443316]
13. Raychaudhuri N et al., PLOS Biol. 10, e1001434 (2012). [PubMed: 23300376]
14. Fitch KR, Yasuda GK, Owens KN, Wakimoto BT, Curr. Top. Dev. Biol 38, 1–34 (1998). [PubMed: 9399075]
15. Dubruille R et al., Curr. Biol 20, 2090–2099 (2010). [PubMed: 21093267]
16. Levine MT, Vander Wende HM, Malik HS, eLife 4, e07378 (2015). [PubMed: 26151671]
17. Yamaki T, Yasuda GK, Wakimoto BT, Genetics 203, 799–816 (2016). [PubMed: 27029731]
18. Binder AM, Wakimoto BT, Davis C, Chmielewski J, Tomkiel Dean JE, Res. J. Dev. Biol 4, 1 (2017).
19. Sandler L, Drosoph. Inf. Serv 47, 68 (1971).
20. Baker BS, Genetics 80, 267–296 (1975). [PubMed: 805757]
21. Von Stetina JR, Orr-Weaver TL, Cold Spring Harb. Perspect. Biol 3, a005553–a005553 (2011). [PubMed: 21709181]
22. Loppin B, Dubruille R, Horard B, Open Biol. 5, 150076 (2015). [PubMed: 26246493]
23. Riparbelli MG, Stouthamer R, Dallai R, Callaini G, Dev. Biol 195, 89–99 (1998). [PubMed: 9520327]
24. Sato M, Tanaka-Sato H, J. Morphol 254, 266–271 (2002). [PubMed: 12386897]
25. Sakai H, Yokoyama T, Tomita S, J. Insect Physiol 139, 104386 (2022). [PubMed: 35358539]
26. Marescalchi O, Zauli C, Scali V, Mol. Reprod. Dev 63, 89–95 (2002). [PubMed: 12211065]
27. Wang L-I et al., J. Cell Biol 220, e202006018 (2021). [PubMed: 33836043]
28. Adams RR, Maiato H, Earnshaw WC, Carmena M, J. Cell Biol 153, 865–880 (2001). [PubMed: 11352945]
29. Horard B, Loppin B, Chromosoma 124, 163–175 (2015). [PubMed: 25563491]
30. Loppin B, Berger F, Annu. Rev. Genet 54, 121–149 (2020). [PubMed: 32857637]
31. Loppin B, Docquier M, Bonneton F, Couble P, Dev. Biol 222, 392–404 (2000). [PubMed: 10837127]
32. Loppin B et al., Nature 437, 1386–1390 (2005). [PubMed: 16251970]
33. Kondo S et al., Genes Dev. 31, 1841–1846 (2017). [PubMed: 29051389]
34. Chen S, Zhang YE, Long M, Science 330, 1682–1685 (2010). [PubMed: 21164016]
35. Rivard EL et al., PLOS Genet. 17, e1009787 (2021). [PubMed: 34478447]
36. Drosophila 12 Genomes Consortium, Nature 450, 203–218 (2007). [PubMed: 17994087]
37. Chang C-H, Mejia Natividad I, Malik HS, eLife 12, e85249 (2023). [PubMed: 36763410]
38. Gao G, Cheng Y, Wesolowska N, Rong YS, Proc. Natl. Acad. Sci. U.S.A 108, 4932–4937 (2011). [PubMed: 21383184]
39. Kimura S, Loppin B, Open Biol. 6, 160207 (2016). [PubMed: 27810970]
40. Tirmarche S et al., G3 4, 2241–2245 (2014). [PubMed: 25236732]

41. Eren-Ghiani Z, Rathke C, Theofel I, Renkawitz-Pohl R, Cell Rep. 13, 2327–2335 (2015). [PubMed: 26673329]
42. Montellier E et al., Genes Dev. 27, 1680–1692 (2013). [PubMed: 23884607]
43. Barral S et al., Mol. Cell 66, 89–101.e8 (2017). [PubMed: 28366643]
44. Arévalo L, Esther Merges G, Schneider S, Schorle H, Reproduction 164, R57–R74 (2022). [PubMed: 35900356]
45. Mann M, Risley MS, Eckhardt RA, Kasinsky HE, J. Exp. Zool 222, 173–186 (1982). [PubMed: 7130928]
46. Oliva R, Dixon GH, Prog. Nucleic Acid Res. Mol. Biol 40, 25–94 (1991). [PubMed: 2031084]
47. Yamauchi Y, Riel JM, Ward MA, J. Androl 33, 229–238 (2012). [PubMed: 21546611]
48. Schmiady H, Kentenich H, Hum. Reprod 4, 689–695 (1989). [PubMed: 2778054]
49. Ooi SL, Priess JR, Henikoff S, PLOS Genet. 2, e97 (2006). [PubMed: 16846252]

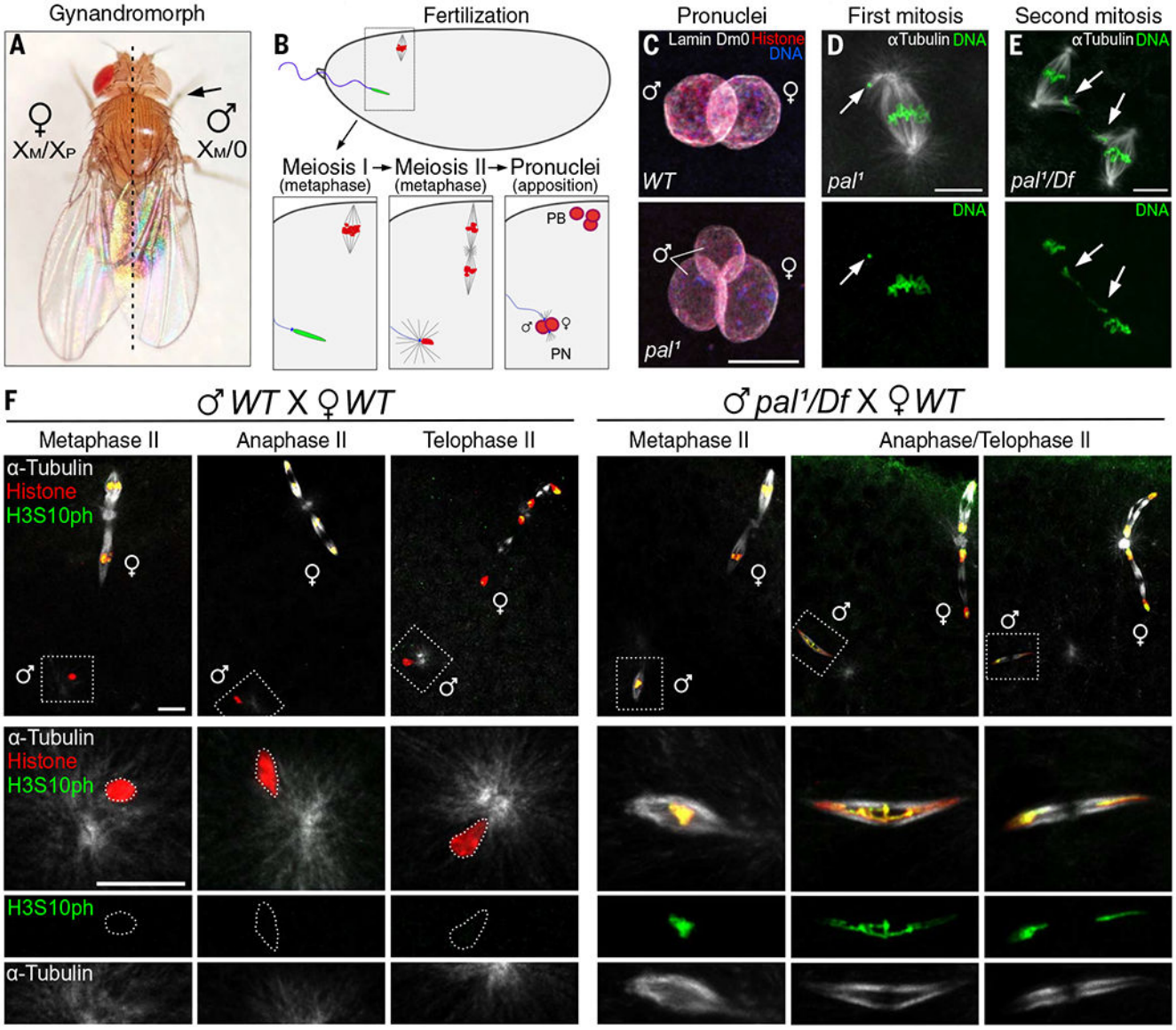

Fig. 1. *pal* induces premature condensation of paternal chromosomes at fertilization.

(**A**) A gynandromorph obtained from a cross between *pal*^{1} males and *w*^{1118} females. Cells in the right half (male) are missing the *white*+ (red eye color) paternal X chromosome (XP) and have only the *white* maternal X chromosome (XM). Note the shorter male wing and presence of sex combs on first leg (arrow). (**B**) Schematic of fertilization and zygote formation in *Drosophila*. Sperm chromatin (green), nucleosomal chromatin (red), microtubules (black), sperm tail, and centrioles (blue). PB, polar bodies; PN, pronuclei. (**C**) (Top) Apposed male and female pronuclei in a control egg. (Bottom) A fragmented male pronucleus in an egg fertilized by *pal*^{1} sperm. WT, wild type. (**D**) A *pal*^{1} embryo during first mitosis with one small chromosome positioned outside the main spindle (arrow). (**E**) Second mitosis in a *pal*^{1}*/Df(2L)ED690* embryo with genetic material scattered between the two spindles (arrows). (**F**) (Left) Control eggs at the indicated phase of female meiosis II. The male pronucleus (inset) remains associated with the sperm aster. (Right)

In *pal*^{1}/*Df(2L)Exel6024* eggs at metaphase of female meiosis II, an ectopic spindle is formed around the male pronucleus, which aberrantly stains for H3S10ph. In anaphase and telophase II, the paternal chromosomes are stretched between the spindle poles. All scale bars, 10 μm.

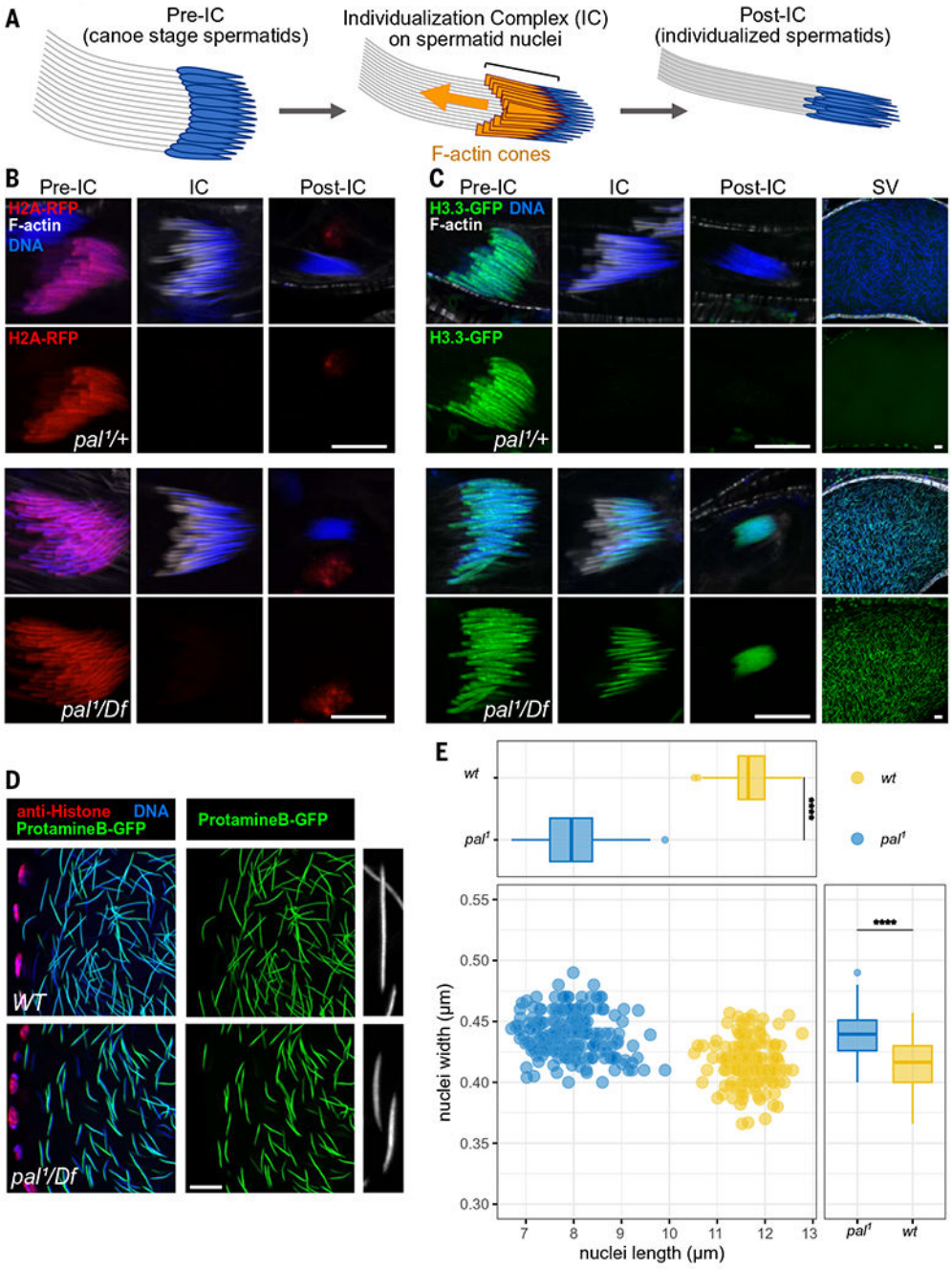

Fig. 2. H3 and H4 are retained in *pal* sperm chromatin.

(**A**) Schematic illustrating the spermiogenesis stages shown in (B) and (C). F-actin cones forming the individualization complex (IC) progress from the anterior end (right) to the posterior end (left) of spermatids. The presence of IC (orange) on spermatid nuclei (blue) indicates the end of the histone-to-protamine transition. (**B**) Confocal images of spermatid nuclei at the indicated stage. In both control (*pal*^{1}/+) and *pal*^{1}/*Df(2L)Exel6024* testes, H2A-RFP is eliminated at the histone-to-protamine transition, before the formation of individualization cones (F-actin). (**C**) H3.3-GFP is eliminated from control spermatids but is

aberrantly retained in *pal*^{1}/*Df(2L)Exel6024* spermatids and mature spermatozoa in seminal vesicles (SV). (**D**) *pal* sperm nuclei incorporate ProtamineB-GFP (ProtB-GFP). Mutant sperm nuclei have aberrant morphology of compared with control sperm nuclei (close-up, right). Scale bars, 10 μm. (**E**) Measurements of sperm nuclear length and width in wild-type (WT) (n = 136) and *pal*^{1} (n = 194) seminal vesicles. t test, ****P < 0.0001.

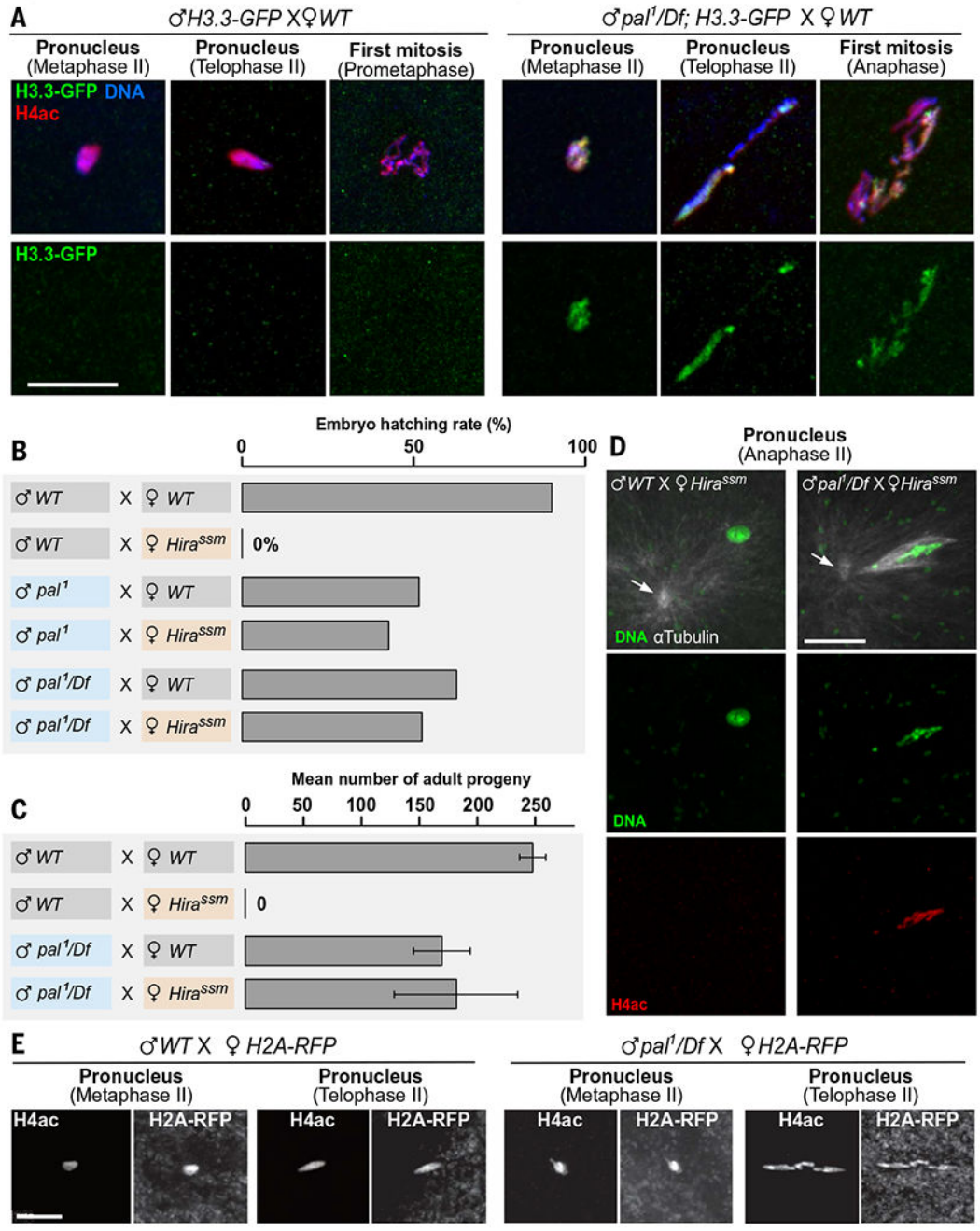

Fig. 3. *pal* sperm rescues *Hira* maternal effect embryo lethality.

(**A**) H3.3-GFP is paternally transmitted by *pal*^{1}*/Df(2L)Exel6024* males and is detected on paternal chromatin during the first mitosis. WT, wild type. (**B**) Percentage of hatched embryos obtained from the indicated crosses. *Df* represents *Df(2L)Exel6024*. (**C**) Mean number (±SD) of F1 adult progeny produced by the indicated crosses. (**D**) In *Hira*^{ssm} control eggs (left), the male pronucleus is round and does not stain for H4ac. In *Hira*^{ssm} eggs fertilized with sperm from *pal*^{1}*/Df(2L)Exel6024* males (right), a spindle forms around paternal chromosomes, which stain for H4ac. Arrows indicate the center of the sperm aster.

Both eggs are infected with the natural endosymbiont *Wolbachia*, which is visible as faint dots in the green channel. (**E**) Maternal H2A-RFP is deposited in paternal chromatin during decondensation of the male pronucleus in both WT and *pal*^{1}*/Df(2L)Exel6024* eggs. All scale bars, 10 μm.

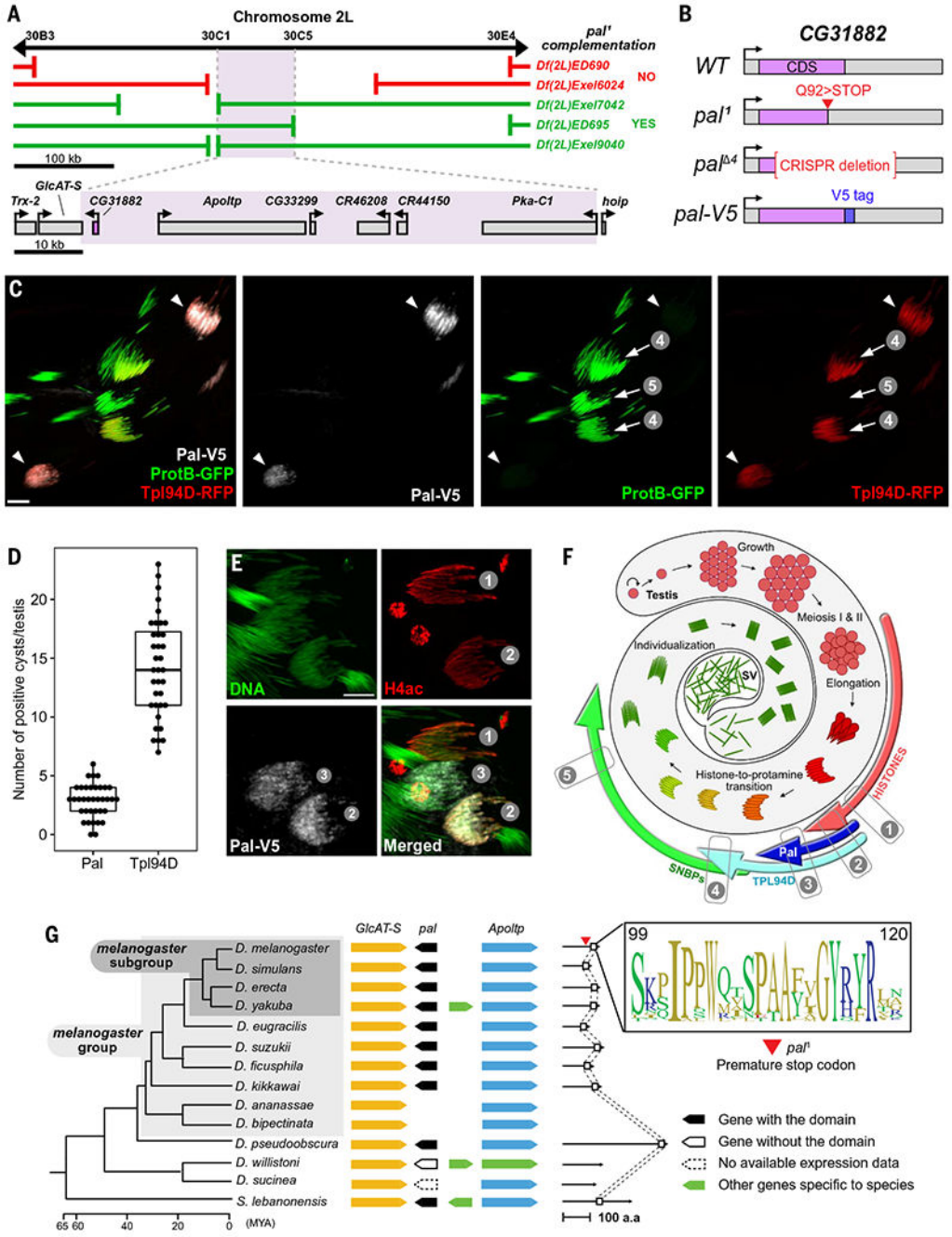

Fig. 4. Pal is a fast-evolving transition protein.

(**A**) Deficiency mapping of *pal*^{1}. The *CG31882/pal* genetic region is shown in purple. (**B**) Schematic of *CG31882/pal* alleles and *pal-V5* rescue transgene. (**C**) Pal-V5 is detected in spermatid nuclei that are positive for Tpl94D-RFP but negative for ProtB-GFP (arrowheads). The numbers in gray circles correspond to the stages defined in (F). (**D**) Quantification of Pal-V5– and Tpl94D-RFP–positive cysts per testis indicates a shorter residency time of Pal in spermatid nuclei. (**E**) Pal-V5 is detected shortly before and after H4ac disappearance. (**F**) Schematic testis that shows the progression of the histone-to-protamine transition. The

stages (one to five) are defined by the presence or absence of indicated chromosomal proteins [see also (C) and (E)]. (**G**) (Left) Representation of *pal* homologs and their neighboring genes, *GlcAT-S* and *Apoltp*, in 13 *Drosophila* species and an outgroup species, *Scaptodrosophila lebanonensis* (subfamily Drosophilinae), whose phylogenetic relationships and divergence times are indicated on the left. There is an apparent absence of a *pal* homolog in *D. ananassae* and *D. bipectinata*. (Right) Pal proteins share a 21-aa conserved C-terminal domain, with relative size of letters indicating aa frequency at each position. Species (nonexhaustive) of the *D. melanogaster* group and subgroup are shown (gray backgrounds).